January, 1992] © 1992 The Chemical Society of Japan Bull. Chem. Soc. Jpn., 65, 129—139 (1992) 129

Electric Field Orientation of Ionizable Polymers with Three Different Electric Dipole Moments. I. New Orientation Function and the Steady-State Electric Birefringence of Poly(L-α-glutamic acid) in Methanolic and Aqueous Solutions

Kiwamu YAMAOKA,* Manabu KIMURA, and Mutsuo OKADA
Faculty of Science, Hiroshima University, 1-3-1 Kagamiyama, Higashi-Hiroshima 724

(Received June 15, 1991)

In order to explain the field strength dependence of the steady-state electric birefringence of ionized poly(L-α-glutamic acid), $(\mathrm{Glu})_n$, in solutions, a new orientation function, $\Phi(\beta,\rho_s,\rho,\gamma')$, was derived on the basis of the permanent dipole, saturable and unsaturable induced dipole (PD–SUSID) moment mechanism. This concept of field orientation is new in that the induced electric moment consists of two parts: One is the saturable induced moment ($\Delta\sigma E$), which transforms to the permanentlike moment ($\Delta\sigma E_0$) at the critical field (E_0), and the other is the unsaturable induced moment ($\Delta\alpha' E$) at any electric fields (E). Some novel features of $\Phi(\beta,\rho_s,\rho,\gamma')$, were graphically illustrated. Comparisons were made between theoretical curves and the birefringence data experimentally measured at 20 °C up to 24 kV cm^{-1} for helical $(\mathrm{Glu})_n$ in pure methanol and in methanol–water (95 : 5 vol%) as well as for coiled $(\mathrm{Glu})_n$ in aqueous solutions (pH 6.9 and 8.0). The degree of dissociation was 0.041 in the former solutions and close to unity in the latter solutions. The field orientation was found to be mostly due to the permanent moment for unionized or slightly ionized $(\mathrm{Glu})_n$, but dominantly due to the saturable induced moment for fully ionized $(\mathrm{Glu})_n$. Appropriate procedures are discussed for estimating the intrinsic birefringence at infinitely high fields.

Studies of the overall conformation and the electric properties of synthetic polypeptides with ionizable side-chain groups are important because the polymers are simple models for natural proteins. The solution properties of high-molecular-weight polypeptides may be unraveled efficiently by the electrooptic methods,[1] among which both electric birefringence and electric dichroism are best known.[1-16] These methods utilize an external electric field to orient molecules along the direction of the field. This field orientation results from the interaction between the electric moments of solutes and the applied electric field.[13,17-23] Three types of electric moments are generally considered for ionized homopolypeptides:[1] (1) the permanent electric dipole moment (μ), for which the main-chain peptide and side-chain polar groups are responsible; (2) the field-induced covalent dipole moment (m_{el} $(=\Delta\alpha E)$), which results from the electronic and atomic polarizability anisotropy ($\Delta\alpha$), and the field-induced ionic dipole moment (m_{ion}). This latter moment should result from the redistribution of counterions bound, either loosely or tightly, to ionizable side chains, e.g., the carboxyl or amino group, upon the application of an external electric pulse field.

The field orientation of ionic polypeptides may be described in terms of an orientation function, in which the interaction energy terms between the above-mentioned electric moments and the field strength (E) are the variables. Once such an orientation function is derived theoretically, the steady-state electric birefringence (Δn) (or the electric dichroism (ΔA)) of rigid and symmetric macromolecular ions may be calculated; hence, the average degree of molecular orientation may be specified at a given field strength. Unfortunately, however, no complete theory is yet available that can predict the orientation behavior of ionized polypeptides.[13,17,19,23] The so-called classical orientation functions have been derived for the unionized symmetric rodlike model by O'Konski et al.[6] and for the disklike model by Shah.[24] (These models possess only permanent and electronic-induced dipole moments (μ and $\Delta\alpha E$)). With those functions the curve-fitting method has extensively been utilized for evaluating both the intrinsic reduced birefringence $(\Delta n/n)_s$ (or the intrinsic reduced dichroism $(\Delta A/A)_s$) at infinitely high fields ($E\rightarrow\infty$) and the two electric moments from the experimental data of polypeptides in the helical conformation in organic solvents.[9,15,25-27] The same procedure was also applied to ionized polymers, simply because the theoretical curves fit reasonably well to observed steady-state birefringence or dichroism values.[6,8,10,11,13,28-33] This procedure should be acceptable only for estimating the intrinsic quantities, on an empirical basis, with no physical meanings being attached to the values of the "electric moments" for ionized polymers.

A new theory was recently advanced by Diekmann et al.[34] and by Yoshioka,[35] who considered that the field-induced ionic electric moment ($\Delta\sigma E$) is saturated at the critical field strength (E_0) and, thereafter, behaves like a permanent dipole moment ($\Delta\sigma E_0$). An extensive comparison was made between the Yoshioka theory[35] and our birefringence data for short, rodlike DNA, which possesses no permanent dipole moment; the agreement was not satisfactory.[36] In order to resolve this difficulty, an assumption was made that the ion-induced electric moment comprises two components: one is the moment, which is not saturated at any electric fields and behaves like an electronic moment (m_{el}), and the other is the moment, which is saturated at E_0 behaving like a permanent dipole at higher fields ($E \geqslant E_0$). The theoretical orientation function ($\Phi(\rho_s, \rho, \gamma')$), designated as the SUSID orientation function, was found to reproduce the field strength dependence of the steady-state birefringence of short DNA fragments well over the entire field region.[36]

The subject of the present work is an extension of the SUSID concept to the field orientation of ionizable polypeptides, which possess the permanent dipole moment, in addition to two other types of electric moments. A new theoretical orientation function, $\Phi(\beta, \rho_s, \rho, \gamma')$, was derived on the basis of the permanent dipole, saturable and unsaturable induced dipole (PD-SUSID) moment mechanism. The result was compared with the experimental electric birefringence data of poly(L-α-glutamic acid), $(\mathrm{Glu})_n$. This homopolypeptide is soluble either in methanol to form an unionized helix,[14,37-39] which becomes partially ionized by the addition of an aqueous sodium hydroxide solution,[39] or in aqueous alkaline solution to form a completely ionized coil.[38,39]

Experimental

Materials. A sample of poly(L-α-glutamic acid), $(\mathrm{Glu})_n$, with a weight-average degree of polymerization of 708 was described previously.[9,14,38] The molecular weight distribution was estimated to be 1.16 in terms of the weight- to number-average weights, M_w/M_n. In order to prepare unionized $(\mathrm{Glu})_n$ in the acid form, the sodium salt of $(\mathrm{Glu})_n$ was dissolved in water and dialyzed exhaustively against dilute HCl at pH 4.1; the solution was then freeze-dried, and finally dried at 78 °C under reduced pressure. The acid form of $(\mathrm{Glu})_n$ was dissolved in absolute methanol, the residue concentration being 1.9 mM (1 M=1 mol dm^{-3}). Partially ionized solutions were prepared by adding 2 mM NaOH aqueous solution to the methanolic solution. The degree of dissociation of the $(\mathrm{Glu})_n$ side-chain carboxyl groups was controlled by adjusting the amount of NaOH added. The final composition of the solvent was kept at 95 (methanol) and 5 (water) in vol%. The backbone conformation of these unionized and partially ionized $(\mathrm{Glu})_n$ was confirmed to be helical up to a 20% dissociation by circular dichroism and by reversing-pulse electric birefringence.[14,39] In order to prepare fully ionized $(\mathrm{Glu})_n$ solutions, the sodium salt ($(\mathrm{NaGlu})_n$) was dissolved in water and the pH was adjusted to 6.9 and 8.0 by adding a NaOH solution, the residue concentration being 1.8 mM.

Measurements. The electric birefringence of $(\mathrm{Glu})_n$ solutions was measured at 20 °C and at 535 nm on an apparatus with a quarter-wave plate, the details of which have been described in previous papers.[9,14,16,38] The electric birefringence (Δn) was expressed with the experimentally determined optical phase retardation (δ); $\Delta n = n_{/\!/} - n_{\perp} = (\lambda/2\pi d)\delta = 2\pi C_v(\Delta g/n)\Phi(E)$, where λ is the wavelength of the incident light, d the pathlength of a Kerr cell, C_v the volume fraction of solute, $\Delta g/n$ the reduced optical anisotropy factor, n the refractive index of solution, and $\Phi(E)$ the orientation factor at E. Experimental techniques for determining these quantities have been given elsewhere.[9,14,16,26,27,33]

Theoretical

Electric Moments. Let an electric moment (m) be induced by an external electric field in a rodlike ionized polymer, which may be approximated by a cylinder or an ellipsoid of revolution possessing the permanent dipole moment (μ). According to the concept already proposed,[36] m is assumed to consist of two parts (m_s and m_u) as shown in Fig. 1, where m_s is the field-induced ionic dipole moment saturable at the critical field strength (E_0), and m_u is the field-induced electronic and/or ionic moment which is unsaturable at any experimentally attainable field strengths. The total electric dipole moment (m_t) associated with an ionized polymer is then given by

$$m_t = \mu + \Delta\alpha' E + \Delta\sigma E, \quad \text{if } 0 \leqslant E \leqslant E_0, \tag{1}$$

and

$$m_t = \mu + \Delta\alpha' E + \Delta\sigma E_0, \quad \text{if } E_0 \leqslant E. \tag{2}$$

Here, $\Delta\alpha' (=\alpha_{33} - \alpha_{11})$ is the covalent and/or ionic polarizability anisotropy responsible for the unsaturable moment ($m_u (=\Delta\alpha' E)$), since both the unsaturable field-induced ionic moment and the electronic moment should behave in the same way toward the applied electric field.[17] $\Delta\sigma (=\sigma_{33} - \sigma_{11})$ is the ionic polarizability anisot-

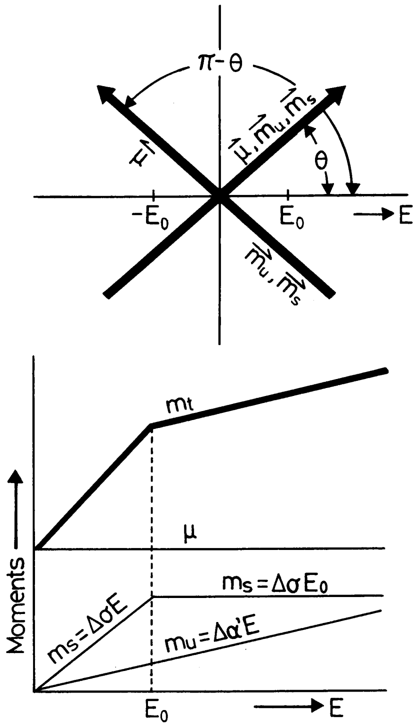

Fig. 1. Electric dipole moments and applied electric field (E) and the angular distribution of dipoles. μ: electric permanent dipole moment; m_s: saturable field-induced ionic dipole moment; m_u: unsaturable field-induced electronic and/or ionic dipole moment; E_0: critical field strength.

ropy responsible for the saturable moment ($m_s(=\Delta\sigma E)$), which is saturated at E_0 to be $\Delta\sigma E_0$. The molecular symmetry axis is designated as the 3-axis and μ has its component only along the 3-axis (i.e., $\mu \equiv \mu_3$).

The potential energy for the interaction between m_t and E is given as (the assumption is made hereafter that $\Delta\alpha' \geqslant 0$ and $\Delta\sigma \geqslant 0$)

$$W = -\mu E - \frac{1}{2}(\Delta\alpha' + \Delta\sigma)E^2, \quad \text{if } 0 \leqslant E \leqslant E_0, \tag{3}$$

and

$$W = -\mu E - \Delta\sigma E_0\, E - \frac{1}{2}\Delta\alpha' E^2 + \frac{1}{2}\Delta\sigma E_0^2, \quad \text{if } E \geqslant E_0. \tag{4}$$

Orientation Functions. Since the procedure has been given elsewhere for the calculation of the SUSID orientation function for an ensemble of ionized polymers,[35,36] the description of the present function is limited to a minimum. The following parameters are introduced:[40]

$$\beta = \mu E/kT,\ \rho_s = 2\gamma_0 E^* = \Delta\sigma E_0 E/kT,\ \rho = \gamma_0 E^{*2} = \Delta\sigma E^2/2kT,$$
$$\gamma' = \Delta\alpha' E^2/2kT,\ \gamma_0 = \Delta\sigma E_0^2/2kT = \rho_s^2/4\rho,\ E^* = E/E_0,$$
$$\text{and } u = \cos\theta, \tag{5}$$

where k is the Boltzmann constant, T the absolute temperature, and θ the angle between the symmetry axis of a polyion and the direction of an applied electric field (cf. Fig. 1). The energy term (W) must be specified by the relative magnitude between E_0 and E; therefore, two cases must be considered separately, i.e., $E^* \geqslant 1$ and $E^* \leqslant 1$.

I. $E_0 \leqslant E\ (E^* \geqslant 1)$, i.e., the field-induced ionic moment is saturated at E_0, which is experimentally attainable. In this case, the energy term (W) must be subdivided into three terms (cf. Eqs. 3 and 4):

(i) if $-E \leqslant E\cos\theta \leqslant -E_0$,

$$W_1 = -(\mu - \Delta\sigma E_0)E\cos\theta - \frac{1}{2}\Delta\alpha' E^2\cos^2\theta + \frac{1}{2}\Delta\sigma E_0^2 \tag{6}$$

(ii) if $-E_0 \leqslant E\cos\theta \leqslant E_0$,

$$W_2 = -\mu E\cos\theta - \frac{1}{2}(\Delta\alpha' + \Delta\sigma)E^2\cos^2\theta \tag{7}$$

(iii) if $+E_0 \leqslant E\cos\theta \leqslant E$,

$$W_3 = -(\mu + \Delta\sigma E_0)E\cos\theta - \frac{1}{2}\Delta\alpha' E^2\cos^2\theta + \frac{1}{2}\Delta\sigma E_0^2 \tag{8}$$

The orientation function Φ contains four parameters (β, ρ_s, ρ, γ') or (β, ρ, γ', E^*), and is given as

$$\Phi(\beta, \rho_s, \rho, \gamma') = \frac{3}{2}\left[\frac{\int_{-1}^{1} u^2 e^{-W/kT} du}{\int_{-1}^{1} e^{-W/kT} du}\right] - \frac{1}{2}$$

$$= \frac{3}{2}\left[\frac{\int_{-1}^{-1/E^*} u^2 e^{-W_1/kT} du + \int_{-1/E^*}^{1/E^*} u^2 e^{-W_2/kT} du + \int_{1/E^*}^{1} u^2 e^{-W_3/kT} du}{\int_{-1}^{-1/E^*} e^{-W_1/kT} du + \int_{-1/E^*}^{1/E^*} e^{-W_2/kT} du + \int_{1/E^*}^{1} e^{-W_3/kT} du}\right] - \frac{1}{2} = \frac{3}{2}\left(\frac{I_4 + I_5 + I_6}{I_1 + I_2 + I_3}\right) - \frac{1}{2}. \tag{9}$$

Integrals I_1—I_6 are complex expressions and are given in **Appendix.**

II. $E_0 \geqslant E\ (E^* \leqslant 1)$, i.e., the field-induced ionic dipole moment is unsaturable at any measurable fields. In this case, the energy term (W) is given over the entire space as

$$W = -\mu E\cos\theta - \frac{1}{2}\Delta\alpha' E^2\cos^2\theta. \tag{10}$$

The orientation function therefore contains parameters β and $(\rho + \gamma')$ and is given as

$$\Phi(\beta, \rho + \gamma') = \frac{3}{2}\left[\frac{\int_{-1}^{1} u^2 e^{-W/kT} du}{\int_{-1}^{1} e^{-W/kT} du}\right] - \frac{1}{2}$$

$$= \frac{3}{4(\rho+\gamma')} \times \left[\frac{e^{\left(\frac{\beta^2}{4(\rho+\gamma')} + (\rho+\gamma')\right)}\left(2\sqrt{\rho+\gamma'}\cosh\beta - \frac{\beta}{\sqrt{\rho+\gamma'}}\sinh\beta\right)}{F\left(\frac{\beta}{2\sqrt{\rho+\gamma'}} + \sqrt{\rho+\gamma'}\right) - F\left(\frac{\beta}{2\sqrt{\rho+\gamma'}} - \sqrt{\rho+\gamma'}\right)} + \frac{\beta^2}{2(\rho+\gamma')} - 1\right] - \frac{1}{2}. \tag{11}$$

This equation is identical to the classical orientation function ($\Phi(\beta, \gamma)$), derived by O'Konski et al. for an unionized polymer, for which $\rho = 0$.[6] It can easily be shown that the new orientation function ($\Phi(\beta, \rho_s, \rho, \gamma')$) reduces to the SUSID function ($\Phi(\rho_s, \rho, \gamma')$), if β is set zero in Eqs. 9—11 and A1—A6 (the polymer possesses no permanent dipole moment).[36] The presently derived $\Phi(\beta, \rho_s, \rho, \gamma')$ will hereafter be called the permanent dipole, saturable and unsaturable induced dipole (PD-SUSID) orientation function.

Results and Discussion

General Behavior of PD–SUSID Orientation Function. Figure 2 shows some theoretical curves for the new PD–SUSID function calculated with Eqs. 9 and 11. The $\Phi(\beta, \rho_s, \rho, \gamma')$ curves are plotted against $(\beta^2+\rho_s^2+2\gamma')$, which is proportional to the second power of field strength, i.e., $[(\mu/kT)^2+(\Delta\sigma E_0/kT)^2+(\Delta\alpha'/kT)]\times E^2$, and is easily compared with experimentally obtained δ values. The parameters are $\beta^2/2\gamma'$ and $\rho_s^2/2\gamma'$, i.e., $(\mu^2/kT\Delta\alpha')$ and $(\Delta\sigma E_0)^2/kT\Delta\alpha'$, representing the relative magnitudes of three electric moments. Since these parameters depend on polypeptides and their conformations, a particular case that $\beta^2/2\gamma'=4$ was plotted. (It is known that values of $\beta^2/2\gamma'$ vary roughly from 2 to 40 for many polypeptides.[1,9,14,16,25–27]) For a comparison, the classical orientation function $(\Phi(\beta, \gamma))$ with a corresponding $\beta^2/2\gamma$ value was also shown (dashed lines). In each Figure, a series of curves were computed by varying another parameter, $\gamma_0(=\Delta\sigma E_0^2/2kT)$. From these Figures, the following four points become clear. (1) All PD-SUSID curves increase monotonically with an increase in the field strength, approaching to the limiting value of unity at infinitely high fields regardless of $\beta^2/2\gamma'$, $\rho_s^2/2\gamma'$, and γ_0. (2) As the ratio of the saturated to unsaturated dipole moments, i.e., $\rho_s^2/2\gamma'$ is increased (a to c), the degree of orientation is lowered at a given field. (3) At constant $\beta^2/2\gamma'$ and $\rho_s^2/2\gamma'$, the theoretical curves depend on γ_0 values; the degree of orientation increases as the saturating field decreases ($\gamma_0<1$), provided that all other conditions remain the same. (4) In some cases, the PD–SUSID curves intersect the classical orientation curves.

Figure 3 shows the new PD–SUSID orientation function normalized by the limiting low-field function (cf. Eq. 15), i.e., $15\Phi(\beta, \rho_s, \rho, \gamma')/(\beta^2+2(\rho+\gamma'))$. The abscissa and other parameters are all the same as in Fig. 2. The ordinate is proportional to the experimental birefringence, (Δn) (or reduced dichroism $\Delta A/A$), normalized by the square of measured electric field strength (E^2). Hence, Fig. 3 is a very useful plot for comparing the experimental data with the PD–SUSID theory. An interesting fact becomes clear from Fig. 3a—c. Under certain conditions, a maximum appears

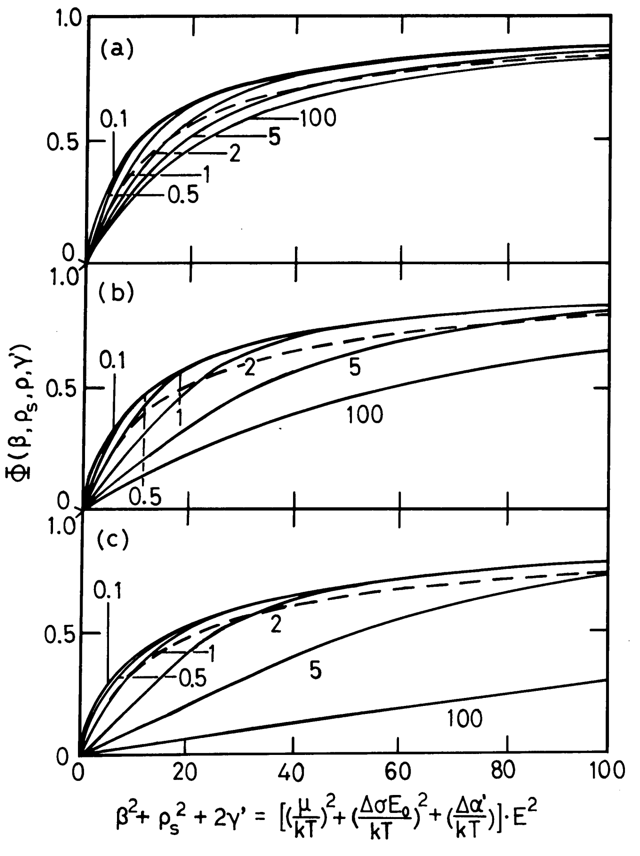

Fig. 2. PD–SUSID orientation functions, $\Phi(\beta,\rho_s^2,\rho,\gamma')$, calculated for a $\beta^2/2\gamma'$ value of 4. The parameter $\rho_s^2/2\gamma'$ is 4(a), 20(b), and 100(c). The numerals in each figure denote values of γ_0. The dashed lines are the classical orientation function, $\Phi(\beta,\gamma)$, calculated for $\beta^2/2\gamma$ of 8(a), 24(b), 104(c).

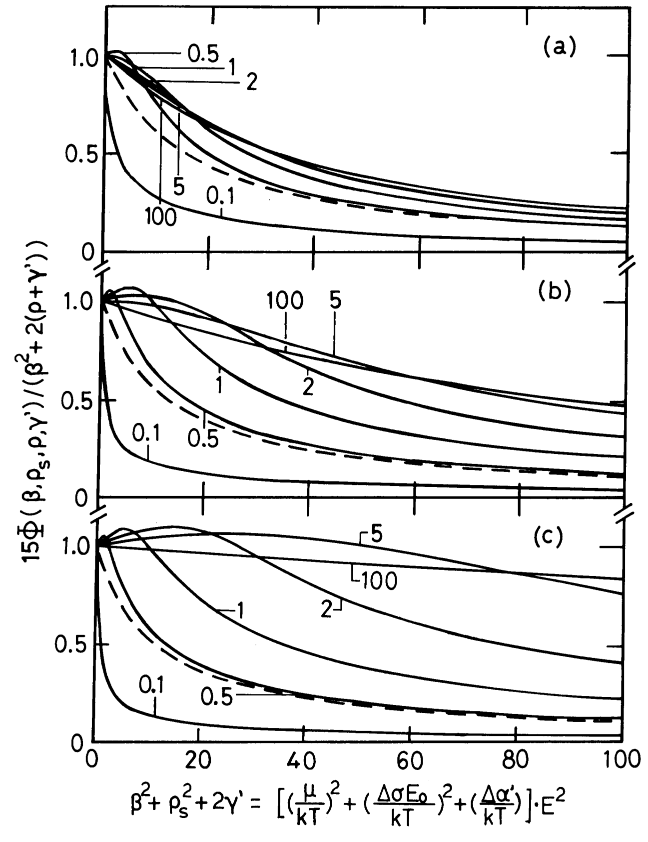

Fig. 3. Normalized PD–SUSID orientation functions, $15\Phi(\beta,\rho_s,\rho,\gamma')/(\beta^2+2(\rho+\gamma'))$ calculated for $\beta^2/2\gamma'$ of 4. The values of $\rho_s^2/2\gamma'$ are 4(a), 20(b), and 100(c). The numerals in each figure denote values of γ_0. The dashed lines are the normalized classical orientation function, $15\Phi(\beta,\gamma)/(\beta^2+2\gamma)$, calculated for $\beta^2/2\gamma$ of 8(a), 24(b), and 104(c).

in the normalized curves. Such a maximum is also known to appear in the classical orientation function for nonionic polymers, if the parameter $\beta^2/2\gamma$ is confined in the range $0 \leqslant \beta^2/2\gamma \leqslant 1.37$.[6] In the SUSID orientation function, a maximum appears at $\rho_s^2/2\gamma'$ values larger than 2.[36] The conditions for the maximum are not so simple as to specify in the present PD–SUSID orientation function, because this function contains three electric dipole moments.

Two Limiting Cases of Field Orientation.

Some approximate but useful orientation functions are derived for both the sufficiently high field region, where molecular orientation is asymptotically completing, and for the Kerr-law region, where the applied electric field is extremely low.

The Sufficiently High Field Region. When the saturable induced ionic moment is saturated at E_0 ($E_0 \leqslant E$), Eqs. 9 and A1—A6 may be expanded asymptotically as

$$\Phi(\beta^2 \gg 1,\ \rho_s^2 \gg 1,\ \gamma' \gg 1) \fallingdotseq 1 - \frac{3}{(\beta+\rho_s)+2\gamma'}. \tag{12}$$

It is interesting to note that Eq. 12 reduces to the approximation derived for the SUSID orientation function at sufficiently high fields (Eq. 16 of Ref. 36), by setting $\beta=0$. If the critical field E_0 is infinitely high, Eq. 11 can be expanded asymptotically as

$$\Phi(\beta^2 \gg 1,\ (\rho+\gamma') \gg 1) \fallingdotseq 1 - \frac{3}{\beta+2(\rho+\gamma')}. \tag{13}$$

This is identical to the approximation derived by O'Konski et al., if no field-induced ionic moment is present ($\Delta\sigma E=0$).[6] Equations 12 and 13 reveal that the orientation function is proportional neither to the reciprocal of the first power of E (the E^{-1}-dependence) nor inversely to the second power of E (the E^{-2}-dependence), if all three electric moments are present in each solute molecule.

Figures 4 and 5 show the plots of $\Phi(\beta, \rho_s, \rho, \gamma')$ against $[\beta^2+\rho_s^2+2\gamma']^{-1}$ or $[(\mu/kT)^2+(\Delta\sigma E_0/kT)^2+(\Delta\alpha'/kT)]^{-1} \times E^{-2}$, i.e., the E^{-2}-dependence, (Fig. 4a—c) and against $[\beta^2+\rho_s^2+2\gamma']^{-1/2}$, i.e., the E^{-1}-dependence (Fig. 5a—c). In each Figure, the solid lines represent the function $\Phi(\beta, \rho_s, \rho, \gamma')$, while the dashed lines are the classical function $\Phi(\beta, \gamma)$. It should be noted that the orientation behavior may be approximated by the classical function only in limited cases. These curves in Figs. 4 and 5, drawn with the same parameters $\beta^2/2\gamma'$, $\rho_s^2/2\gamma'$, and γ_0 as in Fig. 2, clarify the following points: (1) the PD–SUSID theoretical curves generally increase rapidly with a decrease in E^{-2}, each curvature becoming large and approaching the linear portion only asymptotically; (2) the PD–SUSID curves plotted against E^{-1} often show an inverted S-shape curvature, the ceiling or leveling-off trend being remarkable; (3) a simple-minded linear extrapolation of observed δ/cd (or $\Delta A/A$) values to infinitely high fields would undoubtedly produce a considerably underestimated (Fig. 4) or overestimated (Fig. 5) intrinsic $(\delta/cd)_s$ (or $(\Delta A/A)_s$) value. It is clear from Figs. 4 and 5 that the most reliable value of $(\delta/cd)_s$ (or $(\Delta A/A)_s$) should be evaluated by the curve-fitting method, i.e., the fitting of observed δ/cd (or $\Delta A/A$) values to theoretical PD–SUSID curves over a wide range of electric fields.[40]

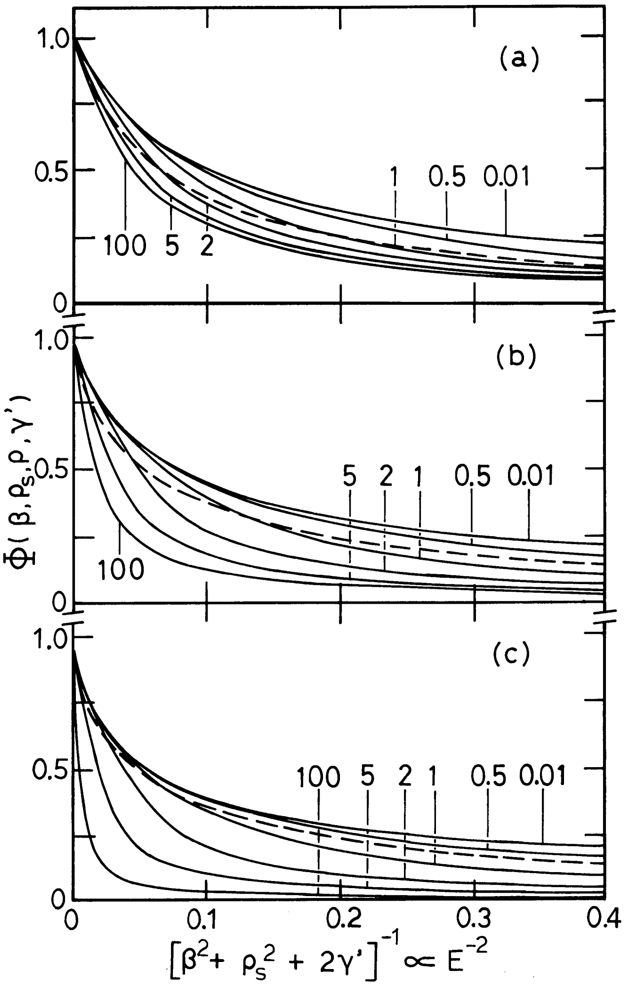

Fig. 4. PD–SUSID orientation function $\Phi(\beta,\rho_s,\rho,\gamma')$ at $\beta^2/2\gamma'=4$ plotted against $[\beta^2+\rho_s^2+2\gamma']^{-1}$. The values of $\rho_s^2/2\gamma'$ are 4(a), 20(b), and 100(c). The numerals in each figure denote values of γ_0. The dashed lines are the classical orientation function at $\beta^2/2\gamma=8$(a), 24(b), and 104(c) plotted against $(\beta^2+2\gamma)^{-1}$.

The Extremely Low-Field Region. If the saturable field-induced ionic moment is sutuated at a very low critical field ($\gamma_0 \to 0$ or $E_0 \to 0$; this is the necessary condition), Eqs. A1—A6 may be expanded to yield the low-field approximation. Then, Eq. 9 is given as

$$\Phi(\beta^2 \ll 1,\ \rho_s^2 \ll 1,\ \gamma' \ll 1) \fallingdotseq \frac{\rho_s}{8} + \frac{\beta^2}{15} + \frac{\rho_s^2}{240} + \frac{2\gamma'}{15}. \tag{14}$$

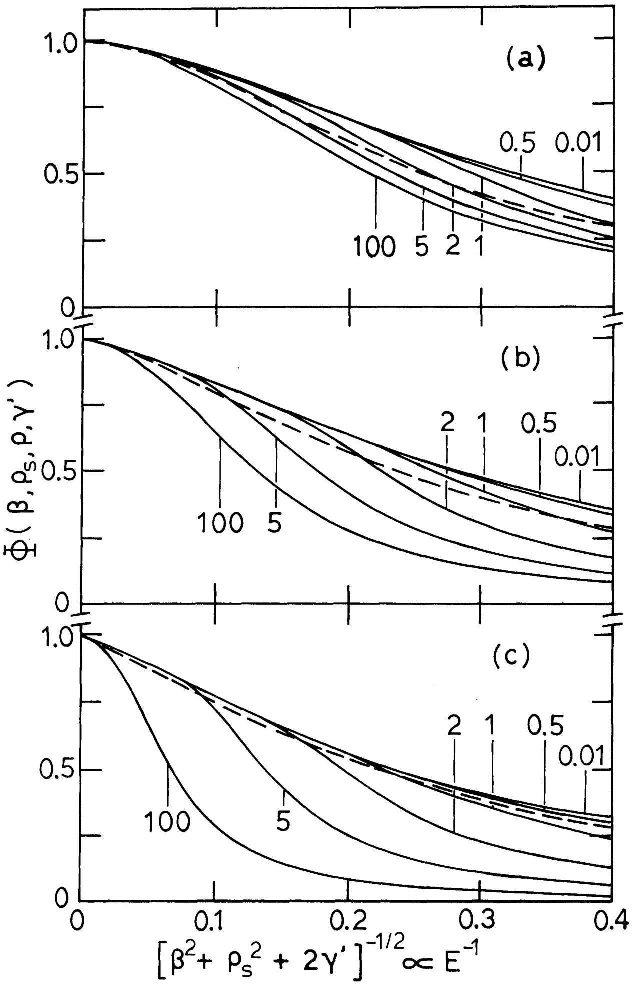

Fig. 5. PD-SUSID orientation function $\Phi(\beta,\rho_s,\rho,\gamma')$ at $\beta^2/2\gamma'=4$ plotted against $[\beta^2+\rho_s^2+2\gamma']^{-1/2}$. The values of $\rho_s^2/2\gamma'$ are 4(a), 20(b), and 100(c). The dashed lines are the classical orientation function at $\beta^2/2\gamma=8$(a), 24(b), and 104(c) plotted against $(\beta^2+2\gamma)^{-1/2}$.

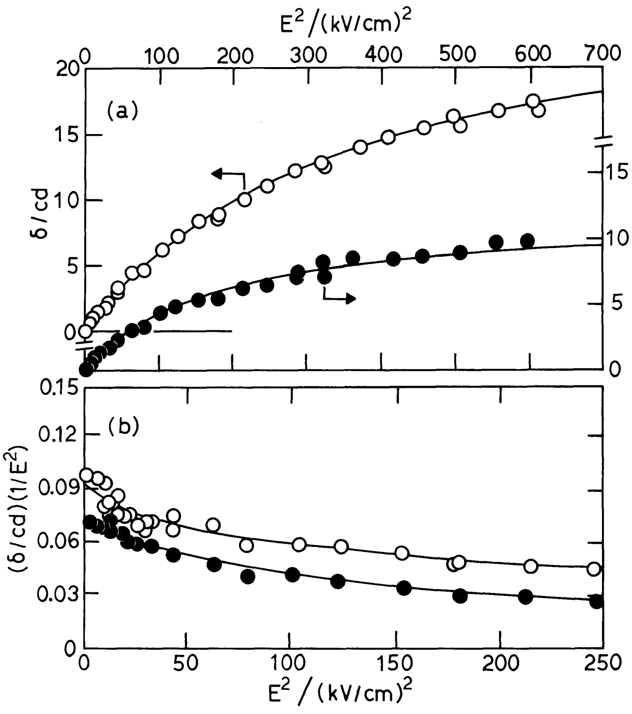

Fig. 6. Field-strength dependence of the steady-state birefringence of $(\mathrm{Glu})_n$ in the helical conformation. (a): the optical phase retardation per residue concentration and pathlength, δ/cd, in deg mM^{-1} cm^{-1}. (b): the same divided by the second power of applied electric field, $(\delta/cd)(1/E^2)$, in deg mM^{-1} cm kV^{-2}. (●): $(\mathrm{Glu})_n$ in pure methanol. (○): $(\mathrm{Glu})_n$ in methanol-water (95:5 vol%) mixed solvent. The solid lines are theoretical orientation functions (see text for details).

On the other hand, if the field-induced moment is not saturated in the low-field region ($E \ll E_0$), Eq. 11 should be expanded as

$$\Phi(\beta^2 \ll 1, (\rho+\gamma') \ll 1) \fallingdotseq \frac{1}{15}(\beta^2+2(\rho+\gamma')). \qquad (15)$$

This expression indicates that the Kerr law (the E^2-law) holds at low fields. On the contrary, Eq. 14 is complicated; the first term is proportional to E (not E^2 !); the following three terms are proportional to E^2. If the field-induced ionic moment is absent ($\Delta\sigma E=0$), Eqs. 14 and 15 reduce to the classical orientation function in the low-field region.[6] If β is set to be zero, Eq. 14 reduces to the SUSID orientation function (Eq. 13 of Ref. 36). Equation 14 reveals an important consequence: the field strength dependence of the steady-state birefringence (or reduced dichroism) would show a non-Kerr law behavior even at low fields, if the saturable ionic moment is saturated at an extremely low field, i.e., $E_0 \rightarrow 0$. In fact, Yamaoka and Charney have already observed that the electric birefringence (Δn) of a high-molecular-weight DNA sample with the Na$^+$ counterion is nearly proportional to the first power of applied fields in the low-field region.[41] The non-Kerr dependence of Δn has also been reported for potassium poly(p-styrenesulfonate)[28] and potassium polyphosphate.[42]

Comparison with Experimental Data of $(\mathrm{Glu})_n$. The PD-SUSID orientation function derived in the preceding sections is now compared with the steady-state birefringence of $(\mathrm{Glu})_n$, which is either in the helical or in the coiled conformation at various degrees of dissociation.

Field Orientation of Helical $(\mathrm{Glu})_n$. Figure 6 shows the steady-state birefringence data in terms of the optical phase retardation (δ) of $(\mathrm{Glu})_n$ in pure methanol and in aqueous methanol (95 vol%), only 4.1% of the side chains being ionized in the latter. The magnitude of δ/cd ($c=$ the residue concentration of $(\mathrm{Glu})_n$ in mM) is larger for the partially ionized $(\mathrm{Glu})_n$ than for the unionized $(\mathrm{Glu})_n$ over the entire field region, though their backbone conformation remains helical.[14,39] Since $(\mathrm{Glu})_n$ is unionized in methanol, the δ/cd vs. E^2 plot (Fig. 6a) was

Table 1. Electrooptical Properties of $(Glu)_n$ Evaluated from Steady-State Electric Birefringence by the PD–SUSID Curve-Fitting Method

Solvent[a)]	pH[b)]	$\beta^2/2\gamma'$	$\rho_s^2/2\gamma'$	γ_0	μ[c)]	$\Delta\alpha'$	$\Delta\sigma$	$\Delta\sigma E_0$[c)]	E_0	$(\delta/cd)_s$
					D	10^{-33}Fm^2	10^{-33}Fm^2	D	kV cm^{-1}	deg mM^{-1} cm^{-1}
MeOH[d)]	— (0)	10	0	—	3300	3.1	0	0	—	12.5
MeOH/H_2O	— (0.04)	5	0.2	0.03	2000	2.2	7.2	400	1.8	27.0
H_2O	6.9 (1.0)	0.01	1.0	0.22	160	7.0	16	1600	3.4	12.8
H_2O	8.0 (1.0)	0.01	1.0	0.25	170	7.9	16	1700	3.6	12.9

a) MeOH for methanol and MeOH/H_2O for methanol–water (95:5 vol%). b) Numerals in parentheses are the degree of dissociation. c) 1 Debye(D)=3.336×10^{-30} C m. d) The parameters are evaluated with the classical function $\Phi(\beta,\gamma)$.

fitted to the classical orientation function,[6)] which is a special case of the PD–SUSID function. The agreement between the experimental plot and the theoretical curve with a $\beta^2/2\gamma$ value of 10 is excellent over the entire field region. The μ value of ca. 3300 Debyes compares favorably with the previously obtained values in other solvents.[9,37)] The δ/cd vs. E^2 plot of the slightly ionized $(Glu)_n$ was fitted to a PD–SUSID function; the use of this function is logical, as was supported by a reversing-pulse electric birefringence study, which revealed the presence of field-induced ionic dipole moment in ionized $(Glu)_n$.[38,39)] All sets of parameters thus evaluated are given in Table 1.

A more stringent test for the orientation mechanism is the plot of observed values of (δ/cd) $(1/E^2)$ against E^2. Figure 6b shows this plot, which emphasizes the low-field behavior of the field strength dependence of steady-state birefringence (cf. Fig. 3). The use of this plot should, therefore, be recommended for detecting the participation of an ionic dipole moment in the field orientation. For the pure methanol solution, the (δ/cd) $(1/E^2)$ *vs.* E^2 plot can be reproduced sufficiently well by the two-parameter classical function. (A better fitting of experimental points to this function may be achieved, if the effect of polydispersity of molecular lengths is considered.[9)] As the side-chain carboxyls are being ionized, the classical function becomes logically unacceptable. The low-field behavior of the partially ionized $(Glu)_n$ is well reproduced with a PD–SUSID function. If the polydispersity effect is taken into account, the fitting is undoubtedly improved, though it is necessary beforehand to clarify the dependence of ion-induced moments ($\Delta\alpha' E$ and $\Delta\sigma E$) on the chain lengths.[9,33,43)] It should be noted that the parameters in Table 1 are less unique for the PD–SUSID than for the classical orientation function, mostly due to the increased number of adjustable parameters (two vs. four).

Field Orientation of Coiled $(Glu)_n$. Figure 7 shows the steady-state birefringence of $(Glu)_n$ in neutral (pH 6.9) and slightly alkaline (pH 8.0) aqueous solutions, where the Glu side chains are nearly completely ionized. The reversing-pulse electric birefringence has shown qualitatively that the contribution of the permanent dipole moment to the electric field orientation is very small in conformity with the coiled backbone structure at pH>7.[10,38)] The orientation is, therefore, due to the ionic moments induced on the polymer chain, which may rather be stiff and extended due to the electrostatic repulsion between ionized carboxyl side chains.[44,45)]

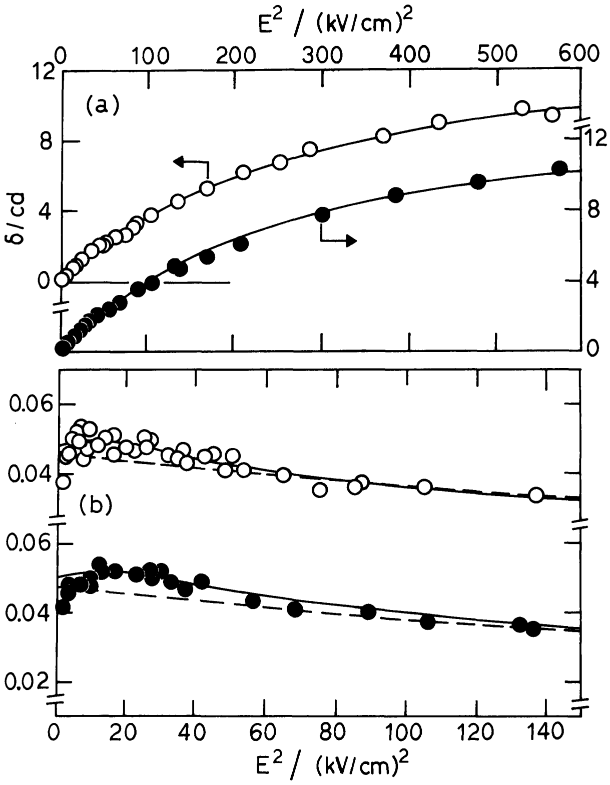

Fig. 7. Field-strength dependence of the steady-state birefringence of $(NaGlu)_n$ in the coiled conformation. (a): δ/cd, in deg mM^{-1} cm^{-1}. (b): $(\delta/cd)(1/E^2)$, in deg mM^{-1} cm kV^{-2}. $(NaGlu)_n$ in water at pH 6.9 (○) and at 8.0 (●). The solid lines are PD–SUSID orientation functions. The dashed lines are the classical orientation function calculated for a $\beta^2/2\gamma$ of 5.

The field strength dependence of observed δ/cd values was fitted to the PD–SUSID orientation functions (Fig. 7a) and the low-field behavior was compared by the (δ/cd) $(1/E^2)$ vs. E^2 plots (Fig. 7b). In the latter plots the observed values show a slight, but distinct, maximum at ca. 3 kV cm^{-1} (pH 6.9) and ca. 4 kV cm^{-1} (pH 8.0). The appearance of such a maximum is predicted by the

PD–SUSID functions (cf. Fig. 3). The experimental plots are well-reproduced over the entire field region with theoretical curves, whose parameters are given in Table 1. Here again, although uniqueness of the evaluated values may be questioned, the general trend is unrefuted. The μ value is twenty-fold smaller for the coiled form than for the helical form. However, the total electric moment (m_t) remains nearly unchanged, being compensated for by the saturated field-induced ionic moment ($m_s=\Delta\sigma E_0$), which amounts to 1600—1700 Debyes, and also by the unsaturable induced ionic moment m_u (a part of $\Delta\alpha' E$). These ionic moments are the main driving force for the field orientation of coiled but ionized (Glu)$_n$. With the PD–SUSID orientation function, therefore, the field strength dependence of the steady-state birefringence of (Glu)$_n$ can be analyzed successfully and significantly; thereby, some useful electric parameters can be evaluated (cf. Table 1).

Intrinsic Birefringence Estimated by Extrapolation to Infinitely High Fields. The main objective of the curve-fitting of observed steady-state birefringence values at higher fields is to evaluate, with least ambiguity, the saturated or intrinsic birefringence Δn_s or $(\delta/cd)_s$ at the complete orientation of solute molecules, which can never be attained experimentally.[20,21,29–33] Figures 8 and 9 show values of δ/cd of (Glu)$_n$ which are plotted against both E^{-2} and E^{-1}. The measured values agree quite well with theoretical curves over the entire field region; the data of three differently ionized (Glu)$_n$ samples were fitted to the PD–SUSID function, while the unionized (Glu)$_n$ to the classical function with parameters evaluated in Figs. 6 and 7 (cf. Table 1). By this curve-fitting method, the important optical property of (Glu)$_n$, i.e., the intrinsic value $(\delta/cd)_s$, could be evaluated with some confidence (Table 1).

Since the unsaturable induced moment ($\Delta\alpha' E$) makes a considerable contribution to the field orientation of (Glu)$_n$ in the helical and coiled conformations (i.e., $\gamma'\neq 0$) regardless of the degress of dissociation, caution must be given about the oft-practised graphical extrapolation to infinitely high fields. Such an extrapolation may yield an overestimated value for $(\delta/cd)_s$, if a linear extrapolation of the observed δ/cd values is carried out

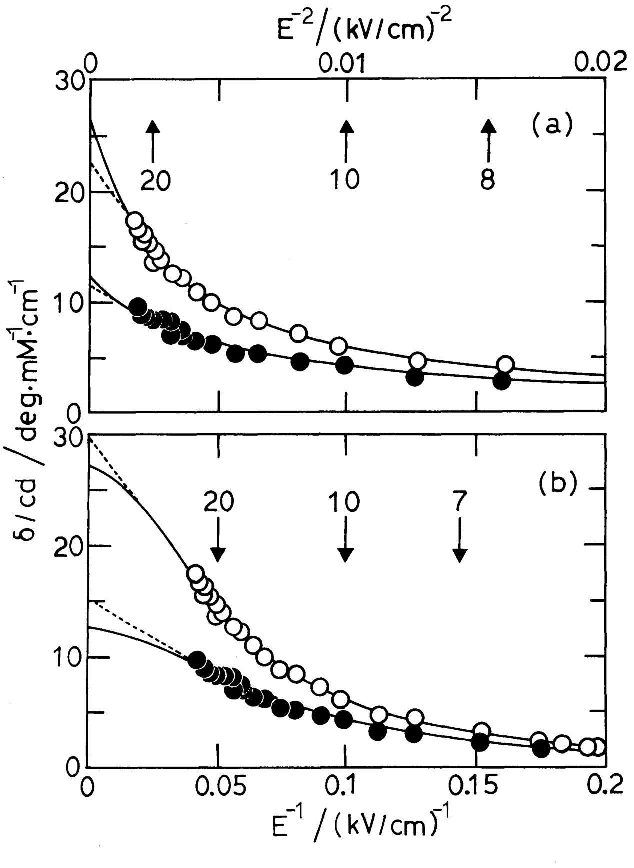

Fig. 8. Extrapolation of observed steady-state birefringence of (Glu)$_n$ in the helical conformation to infinitely high fields. (a): δ/cd vs. E^{-2}. (b): δ/cd vs. E^{-1}. (Glu)$_n$ in pure methanol (●) and in methanol–water (95:5 vol%) mixed solvent (○). The solid lines are the PD–SUSID function, while each dotted line is a linear extrapolation with ten experimental points at higher fields. The numerals in each figure denote the field strength in kV cm^{-1}.

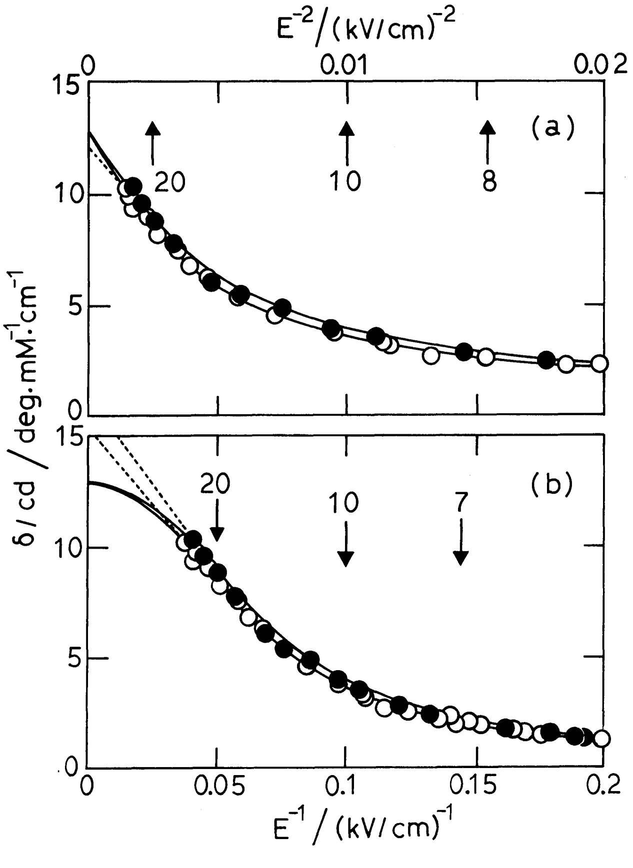

Fig. 9. Extrapolation of the observed steady-state birefringence of (NaGlu)$_n$ in the coiled conformation to infinitely high fields. (a): δ/cd vs. E^{-2}. (b): δ/cd vs. E^{-1}. (NaGlu)$_n$ in water at pH 6.9 (○) and at pH 8.0 (●). Other notations are the same as those in Fig. 8.

against the reciprocal of the first power of field strength E^{-1} over the medium-to-high field region (dotted lines in Figs. 8 and 9). Conversely, an underestimated value would result if the δ/cd vs. E^{-2} plots are extrapolated linearly to infinitely high fields (dotted lines). These trends can be explained by Eqs. 12 and 13, in which two terms, one proportional to E^{-2} (i.e., ρ and/or $2\gamma'$) and the other to E^{-1} (i.e., β and/or ρ_s), are always involved. Whether or not the critical field strength E_0 is present within the attainable field E, a simple linear or nonlinear extrapolation should thus be avoided. The theoretical plots in Figs. 4 and 5 show either a sigmoidal change with an inflection or a sharply increasing curvature. Hence, the curve fitting to PD–SUSID functions is the only reliable means for correctly evaluating the intrinsic value of Δn_s or $(\Delta A/A)_s$.

Concluding Remarks

In order to explain the field strength dependence of steady-state electric birefringence (or dichroism) of ionized homopolypeptides and other related polyelectrolytes with permanent dipole moment, a complete set of orientation functions was derived on the framework of the PD–SUSID mechanism, which constitutes a logical basis for such polymers. Theoretical curves were compared with the experimental steady-state birefringence data of ionized $(\mathrm{Glu})_n$. This curve-fitting method yields a set of four electric quantities (μ, $\Delta\alpha'$, $\Delta\sigma$, E_0) and an optical quantity $(\delta/cd)_s$ or $(\Delta g/n)$. The uniquencess of the first four may somewhat be questioned, but, granting some permissible latitudes to them, they are useful indicators for describing the electric properties of $(\mathrm{Glu})_n$. Since a reversing-pulse electric birefringence study yields additional experimental quantities (the rotational relaxation time, the relative magnitude of μ to $\Delta\alpha'$, the redistribution rate of counterions on the polymer surface, etc.), it would not be difficult to substantiate the numerical values obtained in the present work.[38,39] The effect of polydispersity would also be resolved, once the relationship between the chain length and the saturable ionic electric moment is clarified.[43,45] Introducing the critical field strength E_0 into the SUSID mechanism is somewhat artificial, but is the best compromise between mathematical complexity and operational simplicity.[34–36,43]

We believe that a set of explicit expressions is now available to analyze, on a quantitative basis, the field strength dependence of the electric birefringence and dichroism data of ionized $(\mathrm{Glu})_n$ and other related polymers in the helical and extended-coiled conformations.

We are indebted to Mr. K. Fukudome for his skilled assistance in writing a computer program for the PD–SUSID and classical orientation functions. This work was supported in part by Grant-in-Aid for Scientific Research (A) No. 02405008 from the Ministry of Education, Science and Culture.

Appendix

The integrals (I_1—I_6) are explicitly given as follows:

$$I_1=\int_{-1}^{-1/E^*}\mathrm{e}^{-W_1/kT}\mathrm{d}u=\int_{-1}^{-1/E^*}\mathrm{e}^{(\beta u-\rho_s u+\gamma' u^2-\gamma_0)}\,\mathrm{d}u$$

$$=\frac{\mathrm{e}^{-\gamma_0}\,\mathrm{e}^{-\left(\frac{\beta-\rho_s}{2\sqrt{\gamma'}}\right)^2}}{\sqrt{\gamma'}}\left[F\left(-\frac{\sqrt{\gamma'}}{E^*}+\frac{\beta-\rho_s}{2\sqrt{\gamma'}}\right)\right.$$

$$\left.-F\left(-\sqrt{\gamma'}+\frac{\beta-\rho_s}{2\sqrt{\gamma'}}\right)\right]. \qquad \text{(A1)}$$

$$I_2=\int_{-1/E^*}^{1/E^*}\mathrm{e}^{-W_2/kT}\mathrm{d}u=\int_{-1/E^*}^{1/E^*}\mathrm{e}^{(\beta u+(\rho+\gamma')u^2)}\,\mathrm{d}u$$

$$=\frac{\mathrm{e}^{-\frac{\beta^2}{4(\rho+\gamma')}}}{\sqrt{\rho+\gamma'}}\left[F\left(\frac{\sqrt{\rho+\gamma'}}{E^*}+\frac{\beta}{2\sqrt{\rho+\gamma'}}\right)\right.$$

$$\left.-F\left(-\frac{\sqrt{\rho+\gamma'}}{E^*}+\frac{\beta}{2\sqrt{\rho+\gamma'}}\right)\right]. \qquad \text{(A2)}$$

$$I_3=\int_{1/E^*}^{1}\mathrm{e}^{-W_3/kT}\mathrm{d}u=\int_{1/E^*}^{1}\mathrm{e}^{(\beta u+\rho_s u+\gamma' u^2-\gamma_0)}\,\mathrm{d}u$$

$$=\frac{\mathrm{e}^{-\gamma_0}\,\mathrm{e}^{-\left(\frac{\beta+\rho_s}{2\sqrt{\gamma'}}\right)^2}}{\sqrt{\gamma'}}\left[F\left(\sqrt{\gamma'}+\frac{\beta+\rho_s}{2\sqrt{\gamma'}}\right)\right.$$

$$\left.-F\left(\frac{\sqrt{\gamma'}}{E^*}+\frac{\beta+\rho_s}{2\sqrt{\gamma'}}\right)\right]. \qquad \text{(A3)}$$

$$I_4=\int_{-1}^{-1/E^*}u^2\mathrm{e}^{-W_1/kT}\mathrm{d}u=\int_{-1}^{-1/E^*}u^2\mathrm{e}^{(\beta u-\rho_s+\gamma' u^2-\gamma_0)}\,\mathrm{d}u$$

$$=\frac{\mathrm{e}^{-\gamma_0}\,\mathrm{e}^{-\left(\frac{\beta-\rho_s}{2\sqrt{\gamma'}}\right)^2}}{2(\gamma')^{3/2}}\left\{\left(\sqrt{\gamma'}+\frac{\beta-\rho_s}{2\sqrt{\gamma'}}\right)\mathrm{e}^{\left(\sqrt{\gamma'}-\frac{\beta-\rho_s}{2\sqrt{\gamma'}}\right)^2}\right.$$

$$-\left(\frac{\sqrt{\gamma'}}{E^*}+\frac{\beta-\rho_s}{2\sqrt{\gamma'}}\right)\mathrm{e}^{\left(\frac{\sqrt{\gamma'}}{E^*}-\frac{\beta-\rho_s}{2\sqrt{\gamma'}}\right)^2}$$

$$
+\left[\frac{(\beta-\rho_s)^2}{2\gamma'}-1\right]\left[F\left(-\frac{\sqrt{\gamma'}}{E^*}+\frac{\beta-\rho_s}{2\sqrt{\gamma'}}\right)-F\left(\sqrt{\gamma'}+\frac{\beta-\rho_s}{2\sqrt{\gamma'}}\right)\right]\Biggr\}. \tag{A4}
$$

$$
\begin{aligned}
I_5 &= \int_{-1/E^*}^{1/E^*} u^2 \mathrm{e}^{-W_2/kT}\mathrm{d}u = \int_{-1/E^*}^{1/E^*} u^2 \mathrm{e}^{(\beta u+(\rho+\gamma')u^2)}\,\mathrm{d}u \\
&= \frac{\mathrm{e}^{-\frac{\beta^2}{4(\rho+\gamma')}}}{2(\rho+\gamma')^{3/2}}\Biggl\{\left[\frac{2\sqrt{\rho+\gamma'}}{E^*}\cosh\left(\frac{\beta}{E^*}\right)\right. \\
&\quad \left.-\frac{\beta}{\sqrt{\rho+\gamma'}}\sinh\left(\frac{\beta}{E^*}\right)\right]\mathrm{e}^{\left(\frac{\rho+\gamma'}{E^{*2}}+\frac{\beta^2}{4(\rho+\gamma')}\right)} \\
&\quad +\left(\frac{\beta^2}{2(\rho+\gamma')}-1\right)\left[F\left(\frac{\sqrt{\rho+\gamma'}}{E^*}+\frac{\beta}{2\sqrt{\rho+\gamma'}}\right)\right. \\
&\quad \left.-F\left(-\frac{\sqrt{\rho+\gamma'}}{E^*}+\frac{\beta}{2\sqrt{\rho+\gamma'}}\right)\right]\Biggr\}
\end{aligned} \tag{A5}
$$

$$
\begin{aligned}
I_6 &= \int_{1/E^*}^{1} u^2 \mathrm{e}^{-W_3/kT}\mathrm{d}u = \int_{1/E^*}^{1} u^2 \mathrm{e}^{(\beta u+\rho_s u+\gamma' u^2-\gamma_0)}\,\mathrm{d}u \\
&= \frac{\mathrm{e}^{-\gamma_0}\mathrm{e}^{-\left(\frac{\beta+\rho_s}{2\sqrt{\gamma'}}\right)^2}}{2(\gamma')^{3/2}}\Biggl\{\left(\sqrt{\gamma'}-\frac{\beta+\rho_s}{2\sqrt{\gamma'}}\right)\mathrm{e}^{\left(\sqrt{\gamma'}+\frac{\beta+\rho_s}{2\sqrt{\gamma'}}\right)^2} \\
&\quad -\left(\frac{\sqrt{\gamma'}}{E^*}-\frac{\beta+\rho_s}{2\sqrt{\gamma'}}\right)\mathrm{e}^{\left(\frac{\sqrt{\gamma'}}{E^*}+\frac{\beta+\rho_s}{2\sqrt{\gamma'}}\right)^2} \\
&\quad +\left[\frac{(\beta+\rho_s)^2}{2\gamma'}-1\right]\left[F\left(\sqrt{\gamma'}+\frac{\beta+\rho_s}{2\sqrt{\gamma'}}\right)-F\left(\frac{\sqrt{\gamma'}}{E^*}+\frac{\beta+\rho_s}{2\sqrt{\gamma'}}\right)\right]\Biggr\},
\end{aligned} \tag{A6}
$$

where $F(x)=\int_0^x \mathrm{e}^{t^2}\mathrm{d}t$.

References

1) For reviews, a) C. T. O'Konski, "Encycl. Polym. Sci. Technol.," ed by N. Bikales, Wiley, New York (1968), Vol. 9, pp. 551—590. b) K. Yoshioka and H. Watanabe, "Physical Principles and Techniques of Protein Chemistry, Part A," ed by S. J. Leach, Academic Press, New York (1969), Chap. 7, pp. 335—367. c) E. Fredericq and C. Houssier, "Electric Dichroism and Electric Birefringence," Clarendon Press, Oxford (1973). d) C. T. O'Konski, "Molecular Electro-Optics, Part 1," Marcel Dekker, New York (1976). e) K. Yoshioka, "Molecular Electro-Optics, Part 2," ed by C. T. O'Konski, Marcel Dekker, New York (1978), Chap. 17, pp. 601—643. f) E. Charney, *Q. Rev. Biophys.*, **21**, 1 (1988).

2) The subject has been studied with a variety of electrooptical methods by a great number of workers, since the pulsed techniques were introduced in Refs. 3 and 4; therefore, references are limited hereafter only to those which are closely related to the present work. Numerous references are cited in review articles (Ref. 1).

3) C. T. O'Konski and B. H. Zimm, *Science*, **111**, 113 (1950).

4) H. Benoit, *Ann. Phys. (Paris)*, **6**, 561 (1951).

5) I. Tinoco, Jr., *J. Am. Chem. Soc.*, **79**, 4336 (1957).

6) C. T. O'Konski, K. Yoshioka, and W. H. Orttung, *J. Phys. Chem.*, **63**, 1558 (1959).

7) E. Charney, J. B. Milstien, and K. Yamaoka, *J. Am. Chem. Soc.*, **92**, 2657 (1970).

8) S. Kobayasi and A. Ikegami, *Biopolymers*, **14**, 543 (1975).

9) K. Yamaoka and K. Ueda, *J. Phys. Chem.*, **86**, 406 (1982).

10) K. Yoshioka, M. Fujimori, K. Yamaoka, and K. Ueda, *Int. J. Biol. Macromol.*, **4**, 55 (1982).

11) K. Yamaoka and K. Matsuda, *Macromolecules*, **14**, 595 (1981).

12) K. Yamaoka, and M. Asato, K. Matsuda, and K. Ueda, *Bull. Chem. Soc. Jpn.*, **57**, 1771 (1984).

13) K. Kikuchi, *J. Phys. Chem.*, **88**, 6328 (1984).

14) K. Yamaoka, S. Yamamoto, and K. Ueda, *J. Phys. Chem.*, **89**, 5192 (1985).

15) K. Yamaoka, K. Ueda, and I. Kosako, *J. Am. Chem. Soc.*, **108**, 4619 (1986).

16) K. Yamaoka, S. Yamamoto, and I. Kosako, *Polym. J.*, **19**, 951 (1987).

17) I. Tinoco, Jr. and K. Yamaoka, *J. Phys. Chem.*, **63**, 423 (1959).

18) M. Mandel, *Mol. Phys.*, **4**, 489 (1961).

19) K. Kikuchi and K. Yoshioka, *Biopolymers*, **15**, 538 (1976).

20) D. C. Rau and E. Charney, *Biophys. Chem.*, **14**, 1 (1981).

21) D. C. Rau and E. Charney, *Biophys. Chem.*, **17**, 35 (1983).

22) D. C. Rau and E. Charney, *Macromolecules*, **16**, 1653 (1983).

23) K. Yoshioka, *Prog. Colloid Polym. Sci.*, **68**, 122 (1983).

24) M. J. Shah, *J. Phys. Chem.*, **67**, 2215 (1963).

25) K. Yamaoka, Ph. D. Dissertation, University of California, Berkeley, CA, 1964.

26) K. Ueda, *Bull. Chem. Soc. Jpn.*, **57**, 2703 (1984).

27) K. Ueda, M. Mimura, and K. Yamaoka, *Biopolymers*, **23**, 1667 (1984).

28) K. Kikuchi and K. Yoshioka, *J. Phys. Chem.*, **77**, 2101 (1973).

29) N. C. Stellwagen, *Biopolymers*, **20**, 399 (1981).

30) E. Charney and K. Yamaoka, *Biochemistry*, **21**, 834 (1982).

31) K. Matsuda and K. Yamaoka, *Bull. Chem. Soc. Jpn.*, **55**, 69 (1982).

32) M. Tricot and C. Houssier, *Macromolecules*, **15**, 854 (1982).

33) K. Yamaoka and K. Ueda, *Bull. Chem. Soc. Jpn.*, **56**, 2390 (1983).

34) S. Diekmann, W. Hillen, M. Jung, R. D. Wells, and D. Pörschke, *Biophys. Chem.*, **15**, 157 (1982).

35) K. Yoshioka, *J. Chem. Phys.*, **79**, 3482 (1983).

36) K. Yamaoka and K. Fukudome, *J. Phys. Chem.*, **92**, 2779 (1988).

37) K. Matsumoto, H. Watanabe, and K. Yoshioka, *Biopolymers*, **6**, 929 (1968).

38) K. Yamaoka, T. Ichibakase, K. Ueda, and K. Matsuda, *J. Am. Chem. Soc.,* **102**, 5109 (1980).

39) K. Yamaoka and S. Yamamoto. The detailed result of reversing-pulse electric birefringence of $(\mathrm{Glu})_n$ will be published. Part of this work was presented at the 1st SPSJ International Polymer Conference, Kyoto, Japan, Aug. 1984. *Polym. Prepr. Jpn.,* **1984**, 269.

40) K. Yamaoka and Fukudome, *J. Phys. Chem.,* **94**, 6896 (1990).

41) K. Yamaoka and E. Charney, *Macromolecules,* **6**, 66 (1973).

42) N. C. Stellwagen, Ph. D. Dissertation, University of California, Berkeley, CA, 1967. For review, N. C. Stellwagen, "Molecular Electro-Optics, Part 2," ed by C. T. O'Konski, Marcel Dekker, New York (1978), Chap. 18, pp. 645—683.

43) K. Yamaoka and K. Fukudome, *Bull. Chem. Soc. Jpn.,* **56**, 60 (1983).

44) T. Masujima, K. Yamaoka, and J. Hori, *Bull. Chem. Soc. Jpn.,* **56**, 1030 (1983).

45) K. Yamaoka, K. Ueda, and M. Asato, *J. Am. Chem. Soc.,* **106**, 3865 (1984).